Scientia Horticulturae 339 (2025) 113809

Contents lists available at ScienceDirect

Scientia Horticulturae

journal homepage: www.elsevier.com/locate/scihorti

Research Paper

Proteome and metabolome of *Annona crassiflora* Mart. fruit and their interaction during development

Carlos Alexandre Rocha da Costa [a], Sidney Vasconcelos do Nascimento [b], Rafael Borges da Silva Valadares [b], Luíz Guilherme Malaquias da Silva [a], Gilson Gustavo Lucinda Machado [a], Alice de Paula de Sousa Cavalcante [b], Sayure Mariana Raad Nahon [b], Carlos Henrique Milagres Ribeiro [c], Grécia de Andrade Souza [d], Luiz José Rodrigues [e], Elisangela Elena Nunes Carvalho [a], Eduardo Valério de Barros Vilas Boas [a,*]

[a] *Food Science Department – DCA, Federal University of Lavras – UFLA, Lavras, MG, CEP 37200-900, Brazil*
[b] *Instituto Tecnológico Vale, Rua Boaventura da Silva 955, Belém, PA, CEP 66050-090, Brazil*
[c] *Agriculture Departament – DAG, Federal University of Lavras – UFLA, Lavras, MG, CEP 37200-000, Brazil*
[d] *Biology Department – ICN, Federal University of Lavras – UFLA, Lavras, MG, CEP 37200-000, Brazil*
[e] *Department of Food and Nutrition – DAN, Faculty of Nutrition – FANUT, Federal University of Mato Grosso – UFMT, Cuiabá, MT, CEP 78060-900, Brazil*

ARTICLE INFO

Keywords:
Proteins
Cerrado biome
Maturation
Proteomics
Secondary metabolites
Bioactive compounds

ABSTRACT

Marolo (*Annona crassiflora* Mart.) is an exotic fruit from the Brazilian Cerrado, rich in various bioactive compounds. This unprecedented study analyzed through different techniques (spectrophotometric methods, UPLC, HS-SPME-GC–MS) the proteomic and metabolic changes in four distinct stages of development, their biochemical correlations, biological processes and how proteins are dynamized promoting such processes and biosynthetic pathways. Among the four stages, 993 proteins were identified and 45 metabolites were quantified. At the beginning of development there is a greater presence of ribosomal, transcriptional and post-translational proteins, to increase the protein synthetic machinery that must coordinate the other biological processes essential for development. The families of transcription factors GATA, MADS-Box, MYB, F-box and HD-Zip were identified, which are likely coordinators of the biological processes of marolo together with phytohormones. At the ripe stage, there is an increase in the accumulation of some cellulases to intensify the softening of the fruit, and the antioxidant system of marolo presented a mostly constant behavior, in order to control the steady states of the naturally produced reactive oxygen species. Several proteins identified are related to the detected metabolites, with emphasis on the production and regeneration of vitamin C and the carotenogenic pathway. The volatile profile of marolo was related to the action of some enzymes and the supremacy of volatile esters. Therefore, proteomics in conjunction with metabolomics allowed us to have a molecular view of how compounds and proteins are produced during marolo development and how the behavior of proteins appears to influence biological processes and pathways.

1. Introduction

Marolo (*Annona crassiflora* Mart.), also known as araticum, cerrado pine or ata, is an exotic fruit from the Brazilian Cerrado belonging to the *Annonaceae* family, widely distributed in tropical and subtropical regions, represented by >3000 species (Ramos et al., 2022, 2023). The fruit is a subglobose berry about 11 to 15 cm in diameter and 1 to 2 kg in weight when ripe. Its pulp is yellowish-white in color, due to the presence of carotenoids in its phytochemical composition, and the pulp accounts for 50 % of the fruit's total mass (Carvalho et al., 2022).

* Corresponding author at: Department of Food Science, Laboratory of Postharvest Physiology of Fruits and Vegetables, Federal University of Lavras, Lavras, Minas Gerais, CEP 37200-900, Brazil.
E-mail addresses: alexandre.vitae@gmail.com (C.A.R. da Costa), svn_live@hotmail.com (S.V. do Nascimento), rafael.borges.valadares@itv.org (R.B.S. Valadares), elisangelacarvalho@ufla.br (E.E.N. Carvalho), evbvboas@ufla.br (E.V.B. Vilas Boas).

https://doi.org/10.1016/j.scienta.2024.113809
Received 14 August 2024; Received in revised form 5 November 2024; Accepted 11 November 2024
Available online 28 November 2024

Traditionally in folk medicine, the fruit is used as a tonic and astringent, and indicated to treat pain and rheumatism (Arruda et al., 2023). Along with the various phytochemicals investigated in marolo pulp, such as vitamin C, phenolic compounds, carotenoids, alkaloids and other terpenoids (Almeida et al., 2024), studies have reported the many health-promoting effects associated with these constituents in marolo, such as antioxidant properties (Arruda et al., 2018; Ramos et al., 2023), anti-Alzheimer's (Lucas dos Santos et al., 2018), anticancer (Carvalho et al., 2022), anti-inflammatory (Rosan Fortunato Seixas et al., 2021) and antibacterial (Stafussa et al., 2021; da Silva et al., 2014) activity.

Although marolo is one of the 20 most popular fruits in the Cerrado region, recognized by 85 % of the local population, its harvest for commercial purposes has been carried out in an extractive manner, from native populations, since there are no established commercial crops (Arruda et al., 2023). There are estimates that indicate a significant productivity of *A. crassiflora* Mart., which can reach 400 fruits per hectare in native areas of the Cerrado, with potential for production of up to 2000 fruits per hectare in commercial crops (Almeida et al., 2024). Marolo is consumed fresh or processed, normally as the main ingredient in the composition of several Brazilian regional products, especially sweets. This fruit outstands for its intense and peculiar aroma, nutritional value and functional appeal. However, despite the great value attributed to the fruit of *A. crassiflora* Mart. and its potential for exploitation by the food and pharmaceutical industries and expansion in the international market, this and other native species of the Brazilian Cerrado biome are progressively losing ground in the face of agricultural expansion. In fact, in the last 50 years, more than half of the original vegetation of the Cerrado has been replaced by monocultures and pastures (Fonseca, Uagoda and Chaves, 2021). In this scenario, the use of technological and molecular tools is crucial for the preservation, improvement and expansion of the biotechnological uses of marolo. Researchers have progressively turned to molecular biology technologies, especially genetic tools and omics technologies, such as proteomics and metabolomics, in order to achieve this goal.

Proteomics is a molecular biology technique that systematically and dynamically investigates the variation and accumulation of proteins associated with various biological processes in living beings, organs, tissues or cells (Tian et al., 2024). Metabolomics, in turn, is the systematic study of metabolite profiles, which recognizes and measures small molecules with molecular mass below 1500 Da, in a specific biological or chemical sample (Utpott et al., 2022). Such technologies have played an important role in expanding the understanding of biological processes in fruits and their use has increased the identification of biomarkers, enzyme-substrate interactions, research on bioactivity, exploration of metabolic pathways and understanding of the mechanisms of growth and development of plants and fruits (Li, Wang and Suh, 2022; Momo et al., 2022).

Through these possibilities of molecular and phytochemical characterization, the integration of proteomics and metabolomics has helped in the biochemical understanding of the changes that occur in fruits during the advancement of development and ripening stages (Tartaglia et al., 2024). In tomato, 2607 proteins were more abundant in the ripe fruit than in the ripe green fruit, evidencing an increase mainly in the processes of photosynthesis and interconversions of pentose and glucuronate (Tang et al., 2020). Analyzing four stages of arabica coffee cherries, it was confirmed that the metabolic pathways of amino acids and organic acids are the critical routes in the formation of flavor during ripening (Li et al., 2023c). In three Sorbus stages, the integration of the analyses made it possible to elucidate that most of the differentially abundant proteins are related to the softening process, carbohydrate metabolism and stress responses, and that enzymes abundant in the early stages explain the accumulation of sugars and the reduction of acidity during development (Tartaglia et al., 2024). In white guava, the climacteric ripening behavior was elucidated in addition to the increase in growth regulators during ripening (Monribot-Villanueva et al., 2022). In four pequi stages, the most influential transcription factors acting in the regulation of ripening were members of the MAD-box family (da Costa et al., 2024a).

Therefore, in this present and unprecedented study, we aimed to analyze the proteome and a set of bioactive and volatile metabolites of *A. crassiflora* Mart. fruits at four distinct developmental stages to understand and generate insights into how metabolic changes may have biochemical correlations with the marolo proteome. We also aimed to identify which biological processes occur throughout marolo development and how proteins are dynamized to promote such processes and biosynthetic pathways.

2. Materials and methods

2.1. Harvest, selection and definition of stages

The fruits of *A. crassiflora* Mart. were harvested in a single day in the town of Paraguaçu (21° 33′ 22″ S and 45° 44′ 22″W), southern region of the state of Minas Gerais, Brazil. They were transported, on the same day, to the Post-harvest Fruit and Vegetable laboratory at the Federal University of Lavras, Minas Gerais, Brazil, and sorted into four stages of development, according to the peel and pulp characteristics (Fig. 1).

The marolo is a fruit with no defined description of its development stages, and therefore the description of the stages was processed in two specific ways for this study. The first stage took place in the field with the help of local producers, after a day of research and knowledge exchange. These producers described how they analyze the changes in the fruit, clearly classifying three stages based on external characteristics, which are color and the opening of the peel between the infructescences that together make up the fruit. The second stage was the laboratory evaluation by the research group, analyzing the interior of the fruit together with the overall characteristics of the peel. Both evaluations, by the producers and researchers, were in agreement regarding the definition of the stages and are described below.

In the first stage, called immature, the fruits had a green and extremely rigid peel, and the pulp was firm and whitish. The peel infructescences were very close together, without opening. The overall size of the fruits at this stage is similar to the fruits at the other stages, and is not a differentiating parameter regarding maturation. Marolo fruits present great variability in relation to size. The seeds at this stage presented the same size and dark brown coloration as the other stages. In the second stage, called mature green, the fruits still had predominantly green peel, but with increasing transition to brown, and the peel was softer than the previous stage. The pulp has a color transitioning from white to yellow. The peel infructescences were beginning to open up between themselves. In the third stage, called ripe, the fruit had a soft and brown peel, and the pulp was yellow, juicy and soft. The peel's infructescences had significantly increased the opening between them, a striking characteristic of the fruit considered ripe by producers. The fruits in the last stage, called overripe, were collected on the ground, after natural abscission, with a softer peel texture than in the previous stage, with injuries caused by its fall, which allowed partial visualization of the pulp, yellow in color, less intense than in the previous stage. After removing the peel, the pulps were separated from the seeds manually using stainless steel knives, immediately frozen with liquid nitrogen, placed in polyethylene bags and stored in an ultra-freezer at −80 °C. The pulp of the fruits from each repetition were completely homogenized.

2.2. Proteomics

2.2.1. Freeze drying

Samples were frozen at −75 °C (Coldlab CL 120–86 V, Brazil) for 24 h and then freeze-dried (Edwards, L4KR, Brazil) at −30 °C with a vacuum pressure of 0.998 mbar for 72 h in the dark (Meira et al., 2023). Once freeze-dried, the samples were transported to the Vale Technological Institute, located in the city of Belém (1° 27′ 18″ S, 48° 30′ 9″ W), capital of the state of Pará, northern region of Brazil, where they were

Fig. 1. Four stages of marolo development (*A. crassiflora* Mart).

subjected to proteomic analyses.

2.2.2. Protein extraction and quantification

The proteomic analyses were conducted following the procedure outlined by do Nascimento et al. (2022). The pulp of the fruits were frozen with liquid nitrogen and ground into a fine powder consistency. Each sample received a mixture containing sucrose (1.5 M), Tris-chloride (1.5 M, pH 8), 10 % sodium dodecyl sulfate (SDS), 100 mM methylphenylsulfonyl fluoride (PMSF), polyvinylpolypyrrolidone (PVPP), and ultrapure H_2O. Additionally, 100 µL of protease inhibitor (Protease Inhibitor cocktail - P8340 Sigma-Aldrich) and 500 µL of β-mercaptoethanol were added to each sample. Following five rounds of 30-second sonication, the extracts were split into ten microtubes, each receiving 700 µL of phenol. After vortexing and centrifugation at 14,000 rpm for 8 min twice, the phenolic phase was separated from any remaining aqueous phase or SDS. Finally, 1300 µL of ammonium acetate in methanol were introduced to precipitate the proteins over a period of approximately 24 h at −80 °C. A new round of centrifugation was performed at 14,000 rpm for 8 min, leading to the discarding of the supernatant. The resulting precipitate was then moved to a fresh microtube and rinsed four times with 80 % acetone, followed by a final wash with 70 % ethanol. Subsequently, the precipitate underwent a drying process at room temperature in a vacuum concentrator for around 7 min. The obtained extracts were dissolved in 200 µL of 0.2 % RapiGest (Waters, Milford, MA, USA) and stored for subsequent analysis.

2.2.3. Protein digestion

For the digestion preparation, the proteins were first reduced using dithiothreitol (DTT, 5 mM) and allowed to incubate at 56 °C for 25 min. This step was followed by alkylation with iodoacetamide (IAA, 14 mM) for 30 min. To eliminate any remaining IAA, DTT (5 mM) was added once more and incubated for 15 min. The samples were diluted with a 1:5 ratio of ammonium bicarbonate (50 mM), and CaCl (1 mM) was introduced. The treatment with trypsin (20 ng μL^{-1}) was carried out for 16 h at 37 °C. Next, trifluoroacetic acid (TFA) was introduced to the samples at a final concentration of 0.4 % to halt the enzymatic process. The protein levels in each sample were quantified using the Qubit2.0 fluorometer (Invitrogen, Thermo Fisher Scientific), following the manufacturer's guidelines for the Qubit protein assay kit.

2.2.4. Protein identification and data analysis

Subsequently, five micrograms of peptides were analysed on a NanoACQUITY UPLC ultraperformance liquid chromatography system (Waters, Milford, MA, USA), set up for two-dimensional fractionation. The initial dimension utilized a 5 µm XBridgeTM BEH130 C18 analytical column (300 µm x 50 mm) at a flow rate of 2 µL min^{-1}. The second dimension involved a 5 µm C18 trap column (180 µm x 20 mm) and a 1.7 µm BEH130TM C18 1.8 µm analytical column (100 µm x 100 mm) operated at a flow rate of 400 nL min^{-1}. Samples were fractionated into 5 parts based on a gradient of acetonitrile concentrations: 10.8 %, 14.0 %, 16.7 %, 20.4 %, and 65.0 %. The chromatograph was directly connected to an ESI-Q-ToF Synapt G2S mass spectrometer from Waters set to work in positive mode and continuous fragmentation (MS^E), varying collision energy from 5 to 40 eV Mass spectra were captured within the 50 to 1200 Da range, with a scan time of 0.5 s and an interval of 0.1 s. Peak width and mass spectra resolution were adjusted to automatic mode. The peptide [Glu-1]-fibrinopeptide (lockmass), with a mass of 785.4827 Da and carrying +2 charges, was utilized as a reference and checked every 30 s (following the lockmass spray settings).

Data analysis was performed using Progenesis QI software (Waters) for both identification and quantification, with the Uniprot trembl database from UniProt (UniProtKB/swiss-prot, uniprot.org) used. Protein identification was considered valid when the likelihood of accurately identifying peptides exceeded 90 %, and for proteins, the threshold was set at 95 %. The levels of significance of the proteins with differential abundance were assessed through the ANOVA test (p-value < 0.05) using Progenesis QI. Functional annotation of the proteins was performed with the OmicsBox program version 2.1.14 (Biobam). Principal component analysis (PCA) and a heat map were generated with the Clustvis web tool (https://biit.cs.ut.ee/clustvis/), where the heat map was constructed using the Euclidean distance method. Prediction of protein-protein interaction networks was based on a functional analysis done with STRING software version 12.0 (http://string-db.org/, accessed March 15, 2024), utilizing homologous proteins from *Arabidopsis thaliana* as a reference species.

2.3. Vitamin c and carotenoids

The vitamin C content was determined following the spectrophotometric method outlined by Strohecker & Henning (1967). The extract used was obtained by homogenizing 5 gs of pulp with 45 mL of 0.5 % oxalic acid. After stirring for 30 min, the samples were filtered using quantitative filter paper sized at 15 cm. For the determination, 1 mL of the filtered extract, 3 mL of 0.5 % oxalic acid, 3 drops of 2,6-dinitrophenylhydrazine 2 %, 1 mL of hydrazine and 1 drop of thiourea were added to test tubes. The tubes were placed in a water bath at 37 °C for 3 h, with an ice bath at the end of the period. 5 mL of 85 % sulfuric acid were added to each tube, with the tubes still in an ice bath. After vigorous vortexing and standing for 10 min, the reading was performed at 520 nm. The standard curve was previously obtained with ascorbic acid as

the standard. with the results expressed in mg of ascorbic acid 100 g^{-1}.

Total carotenoids were quantified using the spectrophotometric method described by Rodriguez-Amaya (2001). Initially, 5 gs of sample and 20 mL of cold P.A acetone were added to vials covered with aluminum foil, followed by agitation for 20 min and filtration in Erlenmeyer flasks. The plant material retained on the filter was washed again with acetone until the residue on the paper turned whitish. The filtrate containing the carotenoids extracted in acetone was transferred to separating funnels. In these funnels, 30 mL of petroleum ether and 100 mL of distilled water were added to separate the phases. After the phases were separated, the colorless part was discarded. This procedure was performed 3 times to completely remove the acetone. The remaining extract containing the carotenoids was transferred to 100 mL volumetric flasks, where the volume was completed with petroleum ether. The reading occurred at five absorbances (444 nm = α-carotene; 450 nm = β-carotene; 456 nm = δ-carotene; 462 nm = γ-carotene and 470 nm for lycopene). The following equation was used to determine the carotenoid content:

$$\mu g100g - 1 = \frac{A \times V \times 10^6}{A1cm1\% \times M \times 100}$$

A is the absorbance value obtained, V is the final volume of the solution, A 1cm1 % is the molar absorptivity coeficiente for each carotenoid (2800 = α-carotene; 2592 = β-carotene; 3292 = δ-carotene; 3100 = γ-carotene and 3450 for lycopene). M is the mass of the initial sample. The results were expressed in μg 100 g^{-1}.

2.4. Theobromine, trigonelline and phenolic compounds profile

The technique applied followed the methodology by da Costa et al. (2024a). Falcon tubes with 1 g of *A. crassiflora* Mart. pulp were mixed with 10 mL of 70 % HPLC grade methanol. After shaking for 30 min on a shaker table shielded from light, the samples underwent an additional 30-minute treatment in an ultrasonic bath. Subsequently, the samples were filtered using quantitative filter paper sized at 12.5 cm and a porosity of 0.025 mm. A second filtration step involved a 13 mm diameter membrane filter with a porosity of 0.00022 mm, and a portion of each filtrate was transferred into 1.5 mL vials for injection. High-performance liquid chromatography (HPLC) was carried out in Shimadzu equipment, consisting of a quaternary pump LC-20AT, degasser DGU-20A5, injector SIL-20A, controller CBM-20A, oven CTO-20AC, detector SPDM-20A, detector RID- 10A and fraction collector FRC-10A. The following parameters were adopted: Lc time program: 0.01 min - 0 % B, 5 min - 20 % B; 25 min - 40 % B; 43 min - 45 % B; 50 min - 80 % B; 55 min - 0 % B; 65 min - STOP; Flow: 1 mL min^{-1}; Oven temperature (°C): 35; Injected volume: 0,02 mL; DAD: 280 nm; Shim-pack VP-ODS column 250 mm x 4.6 mm x 0,0005 mm and Shim-pack GVP-ODS pre-column 10 mm x 4.6 mm x 0,0005 mm; Mobile phase A – 2 % solution of glacial acetic acid in ultrapure water; Mobile phase B – Solution consisting of 70 % methanol and 2 % acetic acid in ultrapure water. Fifteen standards were used, namely: trigonelline, theobromine, catechin, resveratrol, vanillin and gallic, chlorogenic, ferulic, caffeic, *o*-coumaric, *m*-coumaric, *p*-coumaric, syringic, rosmarinic and *trans*-cinnamic acids. The results obtained were expressed in mg 100 g^{-1}.

2.5. Volatile compounds

The technique applied followed the methodology by da Costa et al. (2024a). The volatile compounds of the *A. crassiflora* Mart. samples were examined using headspace solid-phase microextraction combined with gas chromatography-mass spectrometry (HS-SPME-GC–MS). Samples weighing 2 g were placed in 20 mL headspace bottles and heated to 40 °C in an aluminum block. Volatile compounds were extracted using a 50/30 μm DVB/CAR/PDMS fiber. Volatile compounds were detected by GC–MS (Shimadzu CG-17 A, Shimadzu, Japan) equipped with an Rtx-5MS column 30 m x 0.25 mm internal diameter x 0.25 μm film thickness (bound phase; 5 % diphenyl, 95 % dimethyl polysiloxane). The carrier gas (helium) flow rate was a constant flow of 1.0 mL min^{-1}. The initial temperature was 40 °C for 30 min, with subsequent ramp rate of column by 3 °C per minute until reaching a temperature of 220 °C. The interface temperature for the MS was 240 °C and the ion source 220 °C. The identification of volatile compounds was based on the comparison of mass spectra using the Willey 8 and NIST libraries.

2.6. Statistic

Data were analysed using the SISVAR 5.8 version software. Analysis of variance (ANOVA) and the Scott-Knott method ($p < 0.05$) were used to compare the possible significant differences among the fruit in four developmental stages. Values were expressed as mean ± standard deviation. The analyses were performed in three replicates per stage. Each replicate was composed of seven fruits, totaling 84 fruits in the study.

3. Results and discussion

3.1. Proteome of A. crassiflora Mart

993 proteins were identified in *A. crassiflora* Mart. fruits during their development (Table S1). Among these, 198 proteins exhibited differential accumulation with statistically significant values at all four stages. These proteins were functionally annotated into 55 biological processes (Fig. 2A). Some proteins were associated with multiple biological processes due to their ability to influence various molecular mechanisms and cellular locations, despite having specific chemical functions and structures. The changes in protein accumulation across stages, represented by proteins that decreased (Fig. 2B) and increased (Fig. 2C), as well as the principal component analysis (PCA) of these 198 proteins among the three replicates at each stage, are also depicted.

The three biological processes that presented the highest amount of proteins were the biosynthesis of organic substances (112), cellular biosynthesis (102), and the metabolic process of organonitrogenous compounds (99). Of these, 68 proteins were common to all processes, and a general heatmap was developed encompassing the three processes (Fig. 3A). Different background colors highlighted proteins common to two processes or exclusive to just one. Fig. 3B presents the analysis of the protein-protein interaction of the proteins described in Fig. 3A, which shows that different types of interactions detected or prospected by public databases can be observed.

In Fig. 3A, it is possible to visualize different clusters formed by the similarity in protein accumulation between stages. In the upper region of the heatmap, a clearly evident cluster is that of proteins most accumulated exclusively in the immature stage. In this cluster, proteins necessary for the translation process stand out. Among these are five ribosomal proteins, 40S ribosomal protein S4, 40S ribosomal protein S18, 40S ribosomal protein S6–2 and two isoforms of 50S ribosomal protein L20. Also in this cluster is the presence of a translation factor, eukaryotic translation initiation factor 5A (eIF5A). Two isoforms of RNA polymerase (EC:2.7.7.6), a transcriptional protein, were also more accumulated in the immature stage. The eukaryotic ribosome, present in the cytosol, is composed of two ribonucleoprotein subunits of unequal sizes, the small 40S subunit and the large 60S subunit (Fakih, Plourde and Germain, 2023), while the chloroplastic ribosome is different, consisting of the 30S and 50S subunits, common to prokaryotes and organelles (Kravchenko et al., 2023). Regarding the main ribosomes in the cytosol, it is in the 40S subunit that mRNA binding occurs at the decoding site, the initial phase of translation, while in the 60S subunit, tRNA molecules catalyze the formation of peptide bonds at the peptidyl transfer site. At the end of translation, the 40S subunit also performs ribosome recycling (Fakih, Plourde and Germain, 2023; Kravchenko et al., 2023). In addition to playing a significant role in ribosome biogenesis, protein synthesis, cell growth, development, apoptosis and

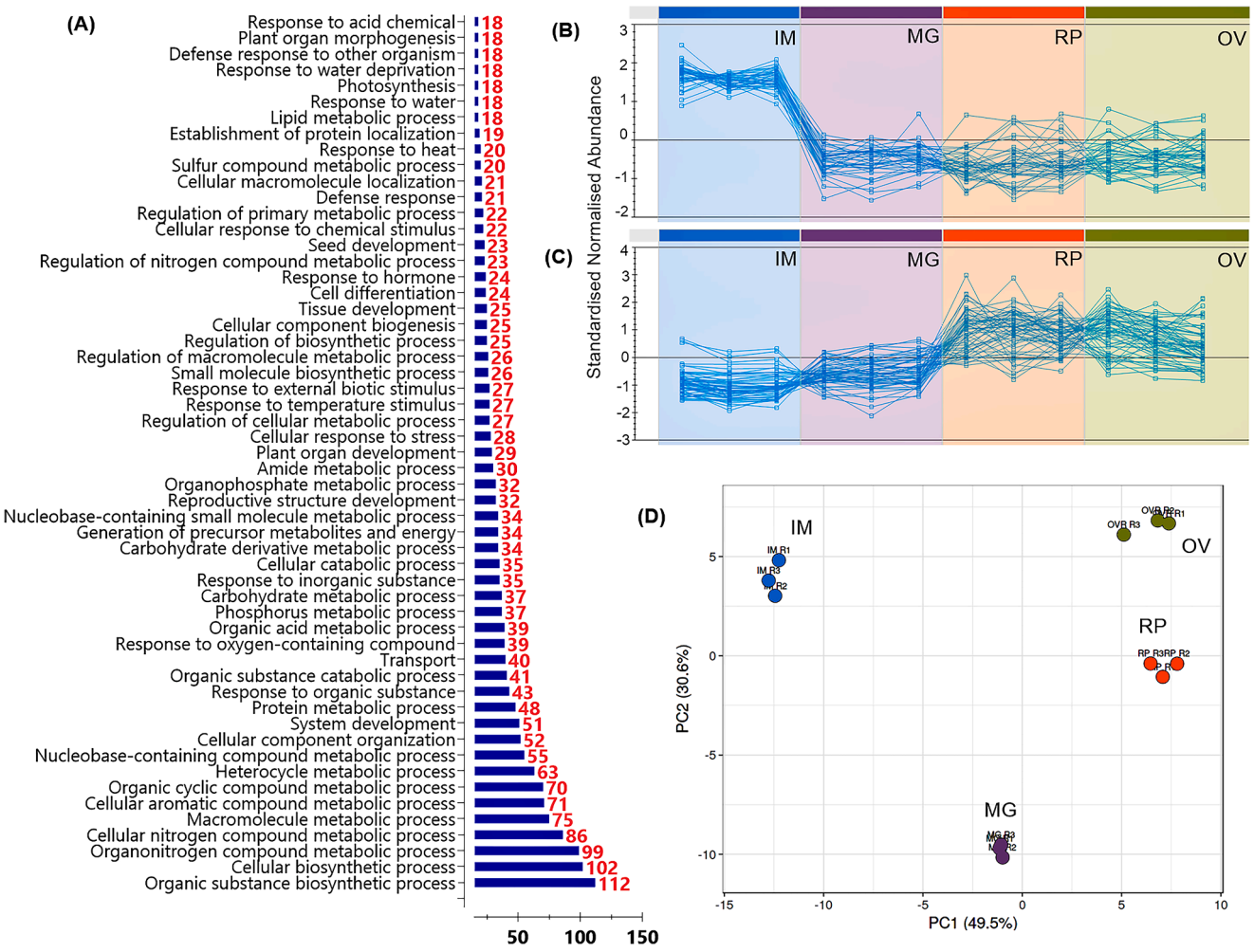

Fig. 2. (A) Functional annotation of biological processes and the respective numbers of proteins for each process. (B) Variation of proteins that decreased in accumulation throughout the stages. (C) Variation of proteins that increased in accumulation throughout the stages. (D) PCA of the four stages of development. Immature (IM), mature green (MG), ripe (RP), and overripe (OV).

maintenance functions, the supply of ribosomal proteins is directly correlated with the rapid growth phase (Saha et al., 2017). eIF5A is a protein that regulates protein synthesis and performs translation elongation and termination as a ribosome quality control cofactor. It also acts by renewing mRNA molecules, in cell proliferation, and in rescuing stalled ribosomes. Its action is reported to be very relevant in the growth of eukaryotic cells, and it has a special peculiarity among eukaryotes, as it is the only protein that contains a rare amino acid, hypusine. Hypusine promotes the activation of eIF5A and its synthesis is directly dependent on the cleavage of spermidine, an important polyamine in climacteric fruits (Park and Wolff, 2018; Pálfi et al., 2021). In the first cluster of Fig. 3A, there is the presence of spermidine synthase 1 (SPDSY1, EC: 2.5.1.16), an enzyme that produces spermidine. Spermidine is a key limiting factor for hypusine synthesis and, consequently, for eIF5A activation. Hypusine synthesis exclusively for eIF5A represents one of the most specific post-translational modifications ever reported in cellular studies (Park and Wolff, 2018). Fig. 3A also shows the proteins eukaryotic initiation factor 4A-9 (eIF4A-9) and 60S ribosomal protein L27, both of which are more accumulated in the immature stage. eIF4A-9 is an initiation factor required for mRNA binding to the ribosome and was accumulated 12.87 times more in the first stage compared to the overripe stage. The combination of these proteins and the behavior of greater accumulation in the first stage shows that one of the most striking events of the immature stage in marolo is the elevation of the cellular machinery that promotes protein synthesis. This must occur to produce more proteins involved in biological processes essential for fruit development. Glycolytic proteins also present at this stage suggest the need for energy production to support all the synthetic processes that tend to increase during fruit development.

As in Fig. 2D, where the immature stage was more distant from the others, in terms of similarity, the first cluster in Fig. 3A, which highlights proteins that were more accumulated in the immature stage, was the largest and most clearly defined among the other clusters. Other smaller clusters in Fig. 3A showed a more dispersed distribution of proteins among the four stages of development of the marolo, with proteins that participate in and regulate distinct routes and reactions. Some of these routes are briefly explained in the topics below.

3.2. Polyamines and S-adenosylmethionine

Polyamines are essential in the regulation of biological processes together with phytohormones, and in the set of most abundant proteins in the first stage of Fig. 3A, another enzyme related to the production of polyamines is Arginase 2 (ARGAH2, EC:3.5.3.1), an enzyme that catalyzes the hydrolysis of arginine into ornithine, subsequently converted into putrescine by the action of Ornithine decarboxylase (ODC, EC:4.1.1.17). ODC was detected in the proteome of marolo in all stages of the fruit, but without statistically significant difference. After the action of ODC, SPDSY1 can then act, converting putrescine into spermidine. Although the function of spermidine as a substrate in the

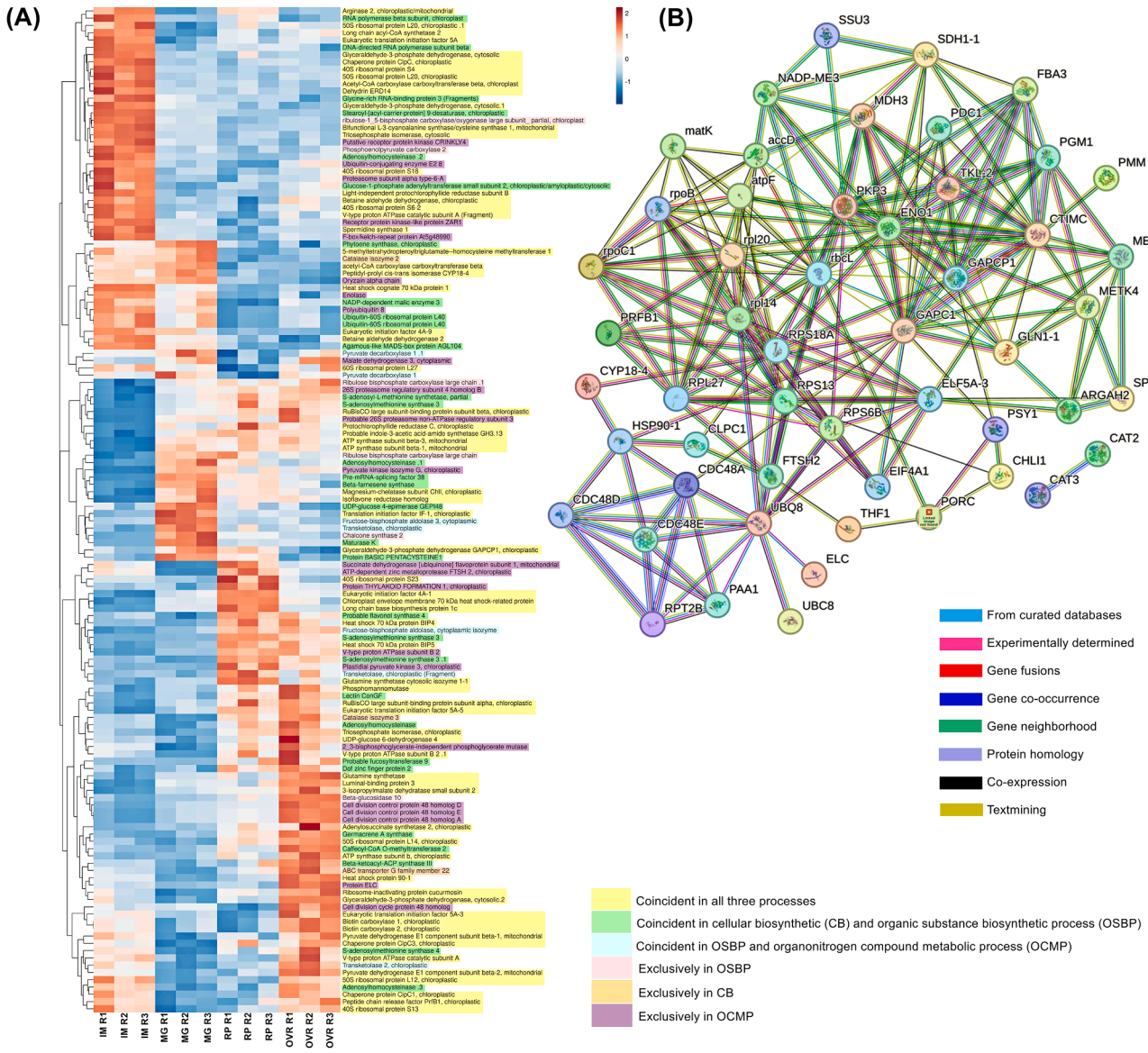

Fig. 3. (A) The heatmap depicts proteins related to the three most prevalent biological processes: organic substances biosynthesis (112), cellular biosynthesis (102), and organonitrogen compounds metabolic process (99) found in the pulp of *A. crassiflora* Mart. across four stages: immature (IM), mature green (MG), ripe (RP), and overripe (OV). Strong red hues indicate high accumulation levels, while deep blue represents lower accumulation. Related to the background colors of the protein names: Yellow: Coincident in all three processes; Green: Coincident in cellular biosynthetic process (CB) and OSBP; Blue: Coincident in OSBP and OCMP; Pink: exclusively in OSBP; Orange: exclusively in CB; Purple: exclusively in OCMP. (B) The protein-protein interactions displayed in the gene list encoding the proteins illustrated in Fig. 3A when compared to equivalent proteins in the *A. thaliana* database. The varying line colors indicate distinct types of recognized or potential interactions.

synthesis of hypusine is reported, most of the spermidine is designated to promote other metabolic processes. Spermidine is an anabolic regulatory molecule, acting as an activation signal for a vast genetic network involved in the regulation of growth and development in fruits (Gao et al., 2021). Therefore, in marolo, the polyamine machinery appears to be more active in the immature stage, aggregating with other development-promoting factors.

The key substrate for polyamine biosynthesis is S-adenosylmethionine (SAM), which is also used for ethylene biosynthesis. Due to the simultaneous occurrence of polyamines and ethylene, there is competition for the same substrate, and depending on the fruit stage, SAM consumption is prioritized between one of these competing pathways (Gao et al., 2021). In marolo, however, 22 different isoforms of S-adenosylmethionine synthase (SAMS), an enzyme that synthesizes SAM, were detected, evidencing an increase in the production of this metabolite to supply the different processes dependent on this substrate. Out of these 22 isoforms observed in marolo, only six showed statistically significant variations among the four stages, all of which exhibited greater accumulation between the third and fourth stages. At the ripe stage, SPDSY1 had the lowest accumulation recorded, allowing the cellular flow of SAM to be directed mainly to ethylene synthesis during marolo ripening. Thus, due to the functions described, the proteins that synthesize polyamines accumulate more in the immature stage to help trigger processes adjacent to fruit development, while in the ripe stage, ethylene must be produced more to intensify the reactions inherent to ripening.

3.3. *Transcription factors*

The process of fruit ripening is controlled by a genetically determined system of plant hormone signaling pathways, which include networks of transcription factors (TFs) and epigenetic modifications that

exert combined and separate effects (Li et al., 2023a). TFs play a role in influencing the expression of various genes encoding proteins involved in different metabolic processes (Li et al., 2022b). Several families of TFs, such as MADS-Box, GATA, F-box, MYB, NAC, ARF, and HD-Zip, have been shown to participate in regulating fruit development and ripening (Forlani, Mizzotti and Masiero, 2021).

A set of proteins from different TF families were detected in the marolo proteome at different developmental stages, with emphasis on the GATA (2), MADS-Box (2), MYB (3), F-box (4), and HD-Zip (5) families. In higher plants, GATA TFs are involved in several biological processes such as response to light, germination, nitrogen metabolism, chloroplast biogenesis, leaf and floral development, phytohormone signaling, and response to many abiotic stresses (Le et al., 2024). However, there are few reports on this family during fruit development. In one of them, GATA TFs, together with F-box and MADS-Box, presented regulatory effects on pepper color formation (Li et al., 2021). Genes from the MYB family, identified in marolo, present pro-carotenogenic activity, in addition to several functions very similar to those of GATA (Yang et al., 2021). MADS-box family TFs are crucial in virtually all aspects of plant growth and development, with evidence indicating that they are particularly influential and central in controlling fruit development and ripening (Liu et al., 2017). MADS-box TFs are engaged in the production of polyphenolic compounds and can act as regulators in the flavonoid and carotenoid pathway (Sánchez-Gómez, Posé and Martín-Pizarro, 2022). The F-box family is one of the most expressive in plants when compared to other eukaryotes. In humans, for example, there are 69 *F-box* genes, while in plants it can exceed 900. Fruits such as apples and pears have 517 and 226 genes from this family, respectively. Due to such diversity, F-box TFs also have broad functions, such as regulating plant growth and development in general, and their action can regulate other TFs, such as MADS-Box (Xu et al., 2021). The HD-Zip family, also found in marolo, follows a similar pattern to the previous superfamilies regarding comprehensive functions in plant growth and development, although they are more closely related to the fruit ripening process when compared to F-box, GATA and MYB TFs. HD-Zip TFs have been correlated with triggering tomato ripening and controlling the ripening process, expression and production of ethylene biosynthesis genes in peach (Lin et al., 2008; Gu et al., 2019).

The individual and joint action of TFs are essential in the development of marolo and in the biosynthesis of various compounds, such as carotenoids and phenolic compounds investigated in this study. The families listed are likely responsible, together with phytohormones, for the central regulation of the development and ripening of *A. crassiflora* Mart. fruits.

3.4. Plant cell wall degradation

One of the most evident physiological changes during fruit ripening and senescence is softening. Biochemically, the polysaccharide networks that make up the plant cell wall are depolymerized by the action of specific enzymes belonging to the cellulase, hemicellulase and pectinase classes.

In the marolo proteome, cellulases stood out with 6 proteins accumulated among all stages, four β-glucosidases (EC: 3.2.1.21) and two endoglucanases (3.2.1.4). The mechanism of enzymatic hydrolysis of cellulose describes the synergistic action of at least three classes of enzymes: endoglucanases, exoglucanases and β-glucosidases or cellobiases. Firstly, endoglucanases act in the internal region of the cellulose fiber, releasing oligosaccharides, while exoglucanases act from the ends of the cellulose, releasing glucose or cellobiose units, and finally, β-glucosidases break the chemical bond that forms cellobiose and oligosaccharides, releasing free glucose units (Sutaoney et al., 2024). Therefore, the action of β-glucosidase is dependent on the above enzymes. Of the six proteins identified, only one endoglucanase and one β-glucosidase showed statistically significant differences between stages. Endoglucanase had maximum and minimum accumulation in the ripe and immature stages, respectively, with a 3.04-fold increase in synthesis between these stages. β-glucosidase showed maximum and minimum accumulation in the overripe and immature stages, respectively, with a 2.24-fold increase in synthesis. It is in the ripe stage that the fruit presents the softening characteristic of the fruit suitable for consumption. Together with the cellulases, three hemicelluloses and one pectate lyase were also identified in the marolo proteome, at practically constant levels during its development. This behavior of the degradative proteins of the cell wall indicates a controlled and measured softening process in the marolo, which is accentuated when the fruit enters the ripe stage, to give it adequate softness. The breakdown of cellulose appears to be the prioritized pathway in marolo. However, the possible role of the aforementioned cellulases in the breakdown of side chains of hemicelluloses and pectins, which contain glucose, cannot be ruled out. The breakdown of these side chains also plays an important role in the softening of fruits.

3.5. Enzymatic antioxidant system

27 Enzymes of the antioxidant system were identified in the marolo proteome, being seven isoforms of superoxide dismutase (SOD, EC 1.15.1.1), 14 isoforms of catalase (CAT, EC 1.11.1.6), one glutathione peroxidase (GPX, EC 1.11.1.9), one glutathione s-transferase (GST, EC:2.5.1.18), three isoforms of monodehydroascorbate reductase (MDHAR, EC:1.6.5.4) and ascorbate peroxidase (APX, EC:1.11.1.11). 18.52 % (five enzymes) of this total showed statistically significant difference between stages. Different processes, such as nitrogen fixation, photosynthesis, respiration and peroxisomal metabolism, constantly generate reactive oxygen species (ROS) from electron transport chains in various organelles (Arias, Feijoo and Moreira, 2022). In order to prevent the toxic accumulation of ROS, plants have developed an antioxidant system that is composed of enzymes and non-enzymatic antioxidant substances, acting as a defense against excess ROS. The oxidative processes involved in the development and ripening of climacteric fruits, such as marolo (da Silva et al., 2013), but also of non-climacteric fruits, result in the production of ROS, which are inevitable byproducts of normal metabolic processes that occur continuously (Huang et al., 2023).

Although they can become toxic if produced uncontrollably, some ROS, such as superoxide radicals and hydrogen peroxide, can play important roles as signaling molecules in cellular processes when present in low concentrations. In these circumstances, antioxidants modulate steady-state concentrations of ROS in order to prevent their toxicity while promoting their beneficial effects. In fruits, antioxidants act to protect tissues against the harmful effects of ROS, reinforcing resistance, preserving nutrients, and extending shelf life after harvest (Huan et al., 2016). Apparently, there were no biotic or abiotic stresses or deregulation of biological processes that could promote oxidative damage in the marolo fruit. Thus, the action of the accumulated antioxidant enzymes probably occurred in controlling the natural production of ROS, with the purpose of keeping them at low levels.

3.6. Vitamin C, carotenoids, alkaloids, phenolic compounds, and enzymes involved in biosynthetic pathways

Changes in the concentrations of the studied bioactive compounds were observed throughout the marolo development (Table 1).

A reduction in vitamin C levels was noted throughout the development of marolo, of the order of 5.7 %, 33.1 % and 41.7 %, in the mature green, ripe and overripe stages, respectively, compared to the immature stage. However, even with such a decrease, ripe fruits, considered ideal for consumption, had a vitamin C content of 96.9 mg 100 g^{-1}. This concentration is higher than that found in oranges, humanity's main source of vitamin C (Randhawa et al., 2020). The Dietary Intake References from the Institute of Medicine (2000) in the United States recommend that for an adult, the dose is 65–90 mg day^{-1}, which suggests

Table 1
Bioactive compounds (mean ± standard deviation) in the pulp of *A. crassiflora* Mart. at four stages of development. Different letters indicate significant differences ($p < 0.05$) by ANOVA analysis followed by the Scott-Knott test. ND – Not Detected.

	Immature	Mature green	Ripe	Overripe
Vitamin C mg of ascorbic acid 100 g^{-1}	144,89^{a} ± 1,99	136,67^{b} ± 0,8	96,9^{c} ± 3,68	84,55^{d} ± 3,77
α-Carotene μg 100 g^{-1}	7,35^{c} ± 0,74	9,53^{b} ± 0,27	14,07^{a} ± 1,23	14,35^{a} ± 2,46
β-Carotene μg 100 g^{-1}	7,94^{c} ± 0,8	10,09^{b} ± 1,02	15,86^{a} ± 1,6	14,73^{a} ± 0,62
δ-Carotene μg 100 g^{-1}	7,26^{b} ± 1,14	7,79^{b} ± 0,74	10,16^{a} ± 1,30	10,69^{a} ± 0,84
γ-Carotene μg 100 g^{-1}	7,7 ^{b} ± 1,21	7,64^{b} ± 0,78	11,2^{a} ± 0,59	10,71^{a} ± 0,89
Lycopene μg 100 g^{-1}	6,35^{b} ± 0,82	8,57^{a} ± 1,79	10,53^{a} ± 0,92	9,63^{a} ± 0,51
Trigonelline mg 100 g^{-1}	12,52^{c}±0,58	14,04^{c}±0,39	26,02^{b}±1,76	61,43^{a}±0,93
Theobromine mg 100 g^{-1}	0,03^{c} ± 0,00	0,06^{b} ± 0,01	0,05^{b} ± 0,01	0,10^{a}± 0,01
Catechin mg 100 g^{-1}	1,18^{b}±0,04	1,01^{b}±0,01	7,99^{a}±0,51	7,62^{a}±0,34
Gallic acid mg 100 g^{-1}	1,66^{c}±0,02	0,89^{d}±0,01	1,89^{b}±0,07	1,95^{a}±0,04
Chlorogenic acid mg 100 g^{-1}	1,57^{d}±0,05	1,91^{c}±0,05	5,72^{a}±0,24	5,31^{b}±0,06
Caffeic acid mg 100 g^{-1}	0,75^{c}±0,04	0,42^{d}±0,02	1,37^{a}±0,03	0,99^{b}±0,02
m-Coumaric acid mg 100 g^{-1}	ND	ND	0,20^{a}±0,02	0,15^{b}±0,01
p-Coumaric acid mg 100 g^{-1}	0,16^{a}±0,00	0,11^{b}±0,01	0,09^{c}±0,00	0,07^{d}±0,01
Rosmarinic acid mg 100 g^{-1}	0,38^{a}±0,03	0,30^{b}±0,02	ND	ND

marolo as an excellent source of this vitamin.

Proteins related to the biosynthesis and recycling pathway of vitamin C, also known as ascorbic acid (AsA) or ascorbate, were detected in the marolo proteome: Phosphomannomutase (PMM, EC:5.4.2.8), Mannose-1-phosphate guanylyl transferase 1 (MPG, EC:2.7.7.13), GDP-mannose 3,5-epimerase (GME, EC:5.1.3.18), three MDHAR isoforms and one APX. PMM, MPG and GME are enzymes of the Smirnoff-Wheeler pathway, the main route of vitamin C synthesis in higher plants (Yu et al., 2021). PMM catalyzes the interconversion of mannose-6-phosphate to mannose-1-phosphate, and MPG converts mannose-1-phosphate to GDP-mannose. Subsequently, through two possible distinct reversible epimerization reactions, GME produces GDP-l-galactose or GDP-l-gulose from GDP-mannose (Dhanalakshmi et al., 2023). Therefore, PMM, MPG, and GME operate sequentially. While PMM varied significantly ($p < 0.05$) throughout development with maximum and minimum accumulation at the overripe and immature stages, respectively, the latter two remained stable ($p > 0.05$). MDHAR and APX are antioxidant enzymes that recycle AsA during their cellular protection action. APX converts AsA to monodehydroascorbate to eliminate H_2O_2, while MDHAR reduces monodehydroascorbate back to ascorbate, regenerating this molecule so that this antioxidant system can occur again (Zheng et al., 2022). Only one MDHAR isoform varied significantly ($p < 0.05$) throughout development with maximum and minimum accumulation in the immature and ripe stages, respectively.

Therefore, the stability of GME and MPG throughout the development and accumulation of PMM in overripe fruits, despite the degradation of vitamin C (Table 1), does not allow us to conclude whether AsA synthesis is reduced in marolo, or whether this antioxidant is still continuously synthesized, but more consumed as the stages advance. It is noteworthy that the intermediates synthesized in the vitamin C synthesis pathway can also be used in the synthesis of sugars incorporated into the cell wall polysaccharides, such as mannose, fucose, galacturonic acid and glucose. This occurs as part of the strategies to strengthen the plant cell wall, which is naturally degraded during fruit ripening and senescence (Nishigaki et al., 2021). The presence of MDHAR and APX isoforms evidences the occurrence of AsA regeneration, a process that provides greater use of the ascorbate available in the fruit.

The concentrations of carotenoids α-, β-, δ-, γ-carotene and lycopene increased significantly ($p < 0.05$) during marolo development, until the fruit reached the ripe stage, no longer changing until the overripe stage (Table 1). This increase is associated with the appearance of the yellowish color of the pulp at the beginning of maturation and its intensification with ripening (Fig. 1). The most abundant carotenoids were β-carotene and α-carotene, reaching concentrations in the ripe fruit of 15.86 μg 100 g^{-1} and 14.07 μg 100 g^{-1}, respectively.

In the marolo proteome, the following proteins related to carotenogenesis were detected: phytoene synthase (PSY, EC:2.5.1.32), three isoforms of farnesyl pyrophosphate synthase (FPS, EC:2.5.1.1), phytoene desaturase (PDS1, EC:1.3.5.5), two isoforms of 4-hydroxy-3-methylbut-2-en-1-yl diphosphate synthase (HMBPPS, EC:1.17.7.1), 4-hydroxy-3-methylbut-2-enyl diphosphate reductase (HMBPPR, EC:1.17.7.4), eight isoforms of pyruvate kinase (PK, EC:2.7.1.40) and nine isoforms of fructose-bisphosphate aldolase (FBA, EC:4.1.2.13).

PK and FBA do not participate directly in the carotenoid synthetic pathway, but are essential for its occurrence. The PK enzyme catalyzes the final step of glycolysis, transferring the phosphate group from phosphoenolpyruvate to ADP, resulting in the production of ATP and pyruvate (Hu et al., 2020). FBA is responsible for catalyzing the reversible aldol cleavage of fructose-1,6-bisphosphate into dihydroxyacetone phosphate and glyceraldehyde-3-phosphate (GAP) (Feng et al., 2020). The interaction between pyruvate and GAP leads to their condensation, and from this process, six successive reactions occur that result in the formation of the isopentenyl pyrophosphate (IPP) molecule, an important precursor of carotenoids in the plastid methylerythritol phosphate (MEP) pathway. HMBPPS and HMBPPR act together in the last two steps preceding the formation of IPP and dimethylallyl diphosphate (DMAPP). HMBPPS converts 2-C-methyl-d-erythritol 2, 4-cyclodiphosphate (ME-2,4cPP) to 1-hydroxy-2-methyl-2-(E)-butenyl 4-diphosphate (HMBPP), and then HMBPPR converts HMBPP to IPP and DMAPP (Krause et al., 2023). Next, two IPP molecules combine with DMAPP to form geranyl diphosphate (GPP), which is subsequently converted to geranylgeranyl diphosphate (GGPP) and is used by PSY in the synthesis of phytoene (Sathasivam et al., 2021). This is the synthesis pathway of tetraterpenes (C_{40}), or higher terpenoids, such as the five carotenoids shown in Table 1.

In addition to being produced in plastids by the MEP pathway, carotenoids can also be synthesized in the cytosol by the mevalonate metabolic pathway (MVA). In this pathway, two IPP molecules condense with DMAPP, through the action of FPS, forming farnesyl pyrophosphate (FPP). FPP is a fundamental branching point of the pathway that can give rise to distinct products, including cholesterol, steroids, dolichols, and all sesquiterpenoids. The range of structures of these latter compounds is subsequently determined by the action of several sesquiterpene synthases (Park et al., 2021; Wang et al., 2022). Therefore, the presence of FPS isoforms in marolo presupposes the synthesis of other compounds, although not monitored in this study.

The aforementioned enzyme PSY plays a key role in carotenoid production, being crucial in the step in which it converts two GGPP molecules into phytoene, the first colorless carotene (Zhou et al., 2022). The subsequent step is the conversion of phytoene into ζ-carotene, carried out by PDS1 (Gou et al., 2024), also found in this proteome. PSY showed minimum and maximum expression in the overripe and mature green stages, respectively, while PDS1 showed no statistically significant difference between the four marolo stages. The enzymes that catalyze the subsequent steps are usually associated with the membrane and are less abundant and, therefore, more challenging to quantify (Cunningham and Gantt, 2007). The peak accumulation of PSY in the

second stage coincides with the increase in carotenoid content between the second and third stages of development. Therefore, its action in the production of tetraterpenes is essential in the chain and failures in the synthesis of PSY would directly result in a deficiency in the pigmentation of the pulp of *A. crassiflora* Mart.

The alkaloids trigonelline and theobromine showed an increase in their concentrations throughout fruit development ($p < 0.05$; Table 1). The maximum trigonelline content was 61.43 mg 100 g^{-1}, while theobromine was 0.1 mg 100 g^{-1}, both in overripe fruit. Alkaloids, such as trigonelline and theobromine, are compounds that have in common a heterocyclic ring containing an N atom (da Costa et al., 2023). An essential enzyme found to be active in the production of trigonelline was SAMS. This enzyme synthesizes SAM as a metabolite, which interacts with nicotinic acid to supply methyl groups needed for trigonelline synthesis (Ashihara, 2015).

SAMS isoforms with statistically significant variations showed greater accumulation between the third and fourth stages. The most significant rise in trigonelline, a 2.36-fold increase, happened between these two stages. A probable bottleneck enzyme implicated in the production of trigonelline in marolo is aspartate aminotransferase (AspAT, EC:2.6.1.1), responsible for deaminating aspartate into oxaloacetate, a crucial component for malate production utilized in the mitochondria for the tricarboxylic acid cycle (Han et al., 2021). Aspartate serves as the starting material for the trigonelline synthesis pathway (Ashihara, 2015). Three AspAT isoforms were detected, but none with statistically significant differences between stages of development.

Of the 13 phenolic compounds assessed, seven were detected in marolo. In general, there was an increase in the concentrations of catechin and gallic, chlorogenic and caffeic acids and a drop in the concentrations of *m*-coumaric, *p*-coumaric and rosmarinic acids during the fruit's development. It should be noted that *m*-coumaric acid was only identified in ripe and overripe fruit, while rosmarinic acid was identified in immature and mature green fruits. The other phenolics were identified in the fruit at all stages.

Among the enzymes identified in the proteome of *A. crassiflora* Mart. fruits, related to the biosynthetic pathways of phenolic compounds, those of the flavonoid pathway stand out, with 14 specific representatives. Catechin (Table 1) is a flavonoid of the proanthocyanidin class, and was the most abundant phenolic compound observed in this study, reaching a content of 7.99 mg 100 g^{-1} in the ripe fruit. From the group of 14 proteins, five isoforms of chalcone synthase (CHS, EC:2.3.1.74) were identified. CHS is the major and first rate-limiting enzyme in the flavonoid biosynthetic pathway and generates the central metabolite of the flavonoid branch classes, the chalcone naringenin (Liu et al., 2021). The other flavonoid pathway-specific enzymes were three isoforms of flavonol synthase (FLS, EC:1.14.20.6), Flavonol 3-O-glucosyltransferase UGT89B1 (EC:2.4.1.91), two isoforms of Chalcone–flavanone isomerase (CHI, EC:5.5.1.6), and three isoforms of Isoflavone reductase homolog (EC:1.3.1.). In strawberry, *CHS, CHI* and *FLS* genes were upregulated by the action of MADS-Box and MYB TFs (Sánchez-Gómez, Posé and Martín-Pizarro, 2022).

The reduction in chlorogenic and caffeic acids in overripe fruits may be due to degradation resulting from the onset of senescence. Related to caffeic acid, three Caffeoyl-CoA O-methyltransferases (CCoAOMT, EC:2.1.1.104) and one Caffeic acid 3-O-methyltransferase (COMT, EC:2.1.1.68) were detected in the proteome at all developmental stages of marolo. COMT is responsible for converting caffeic acid to ferulic acid, while CCoAOMT methylates caffeoyl-CoA (a metabolite generated directly from caffeic acid) to feruloyl-CoA and 5-hydroxyferuloyl-CoA to sinapoyl-CoA (Luo et al., 2022). Therefore, only CCoAOMT can obligatorily act when caffeic acid has been converted to caffeoyl-CoA. Only one CCoAOMT isoform showed significant variations in its levels among the four development stages, with maximum and minimum accumulation in the overripe and mature green stages, respectively. The lowest accumulation, observed in the mature green stage, coincided with a 3.3-fold increase in caffeic acid concentration between the second and third development stages. The highest accumulation, observed in the overripe stage, coincided with a reduction in caffeic acid, the immediate precursor of the CCoAOMT substrate. This enzyme is important in strengthening the plant cell wall, being related to the response to wounds or entry of pathogens by increasing the formation of feruloylated polysaccharides bound to the wall (Lepelley et al., 2007). The accumulation of CCoAOMT in the overripe stage can be understood as a defense mechanism, at a stage in which the fruit is highly stressed, weakened and susceptible to microbiological deterioration. To contain the advance of senescence or invaders, molecular strategies such as the action of CCoAOMT and other enzymes that act for this purpose naturally undergo positive regulation. As for the other phenolic compounds studied, proteins directly responsible for their synthesis were not detected in the proteome of *A. crassiflora* Mart. However, their presence suggests health-promoting effects of the marolo, since they are phytochemicals with well-defined bioactive effects (da Costa et al., 2024b; Marcolino et al., 2024).

3.7. Volatile organic compounds (VOC) and related proteins

30 VOC were identified among the four stages of *A. crassiflora* Mart. Such VOC are presented in Table 2 with their respective percentages of area per stadium.

VOC are crucial elements that enhance the quality and appeal of fruits to both animals and humans. These fragrant substances are characterized by their high vapor pressure, moderate hydrophilicity, and low molecular mass. The distinctive smell of food is determined by the combined perception of its volatile profile (Jiménez-Bremont et al., 2024). The composition of VOC changes throughout the ripening process, and they are produced from amino acid derivatives, sugars, and fatty acid compounds (Li et al., 2022a; Mostafa et al., 2022).

The ester class was the most abundant in the volatile profile of marolo with 17 compounds, representing 51 % of the identified compounds. Next, the class with the most elucidated representatives was terpenes with 5 VOC. The major compounds identified in marolo were ethyl octanoate (33.85 % in overripe fruits), ethyl hexanoate (32.24 % in ripe fruit) and methyl octanoate (21.64 % and 22.02 % for the immature and mature green stages, respectively), all esters. Esters have mainly fruity notes, and in fruits they are the largest group of volatiles synthesized through the esterification of alcohols and acyl CoA derived from the metabolism of fatty acids and amino acids. This reaction is catalyzed by alcohol acyltransferase (Mostafa et al., 2022). Individual esters can act in a coordinated and integrated way, forming what can be identified as an aroma vector. Even with small changes in concentration, very significant changes in flavor perception and intensity can be detected according to the combination of different types and concentrations of esters (Xu et al., 2022).

Proteins involved in the production of volatile esters were detected in the proteome of marolo at all fruit stages: one Linoleate 13S-lipoxygenase 2–1 (LOX2.1, EC: 1.13.11.12) and five isoforms of alcohol dehydrogenases (ADH, EC: 1.1.1.1). Of these, only one ADH isoform varied significantly ($p < 0.05$) throughout development, with minimum and maximum accumulation in the immature and overripe stages, respectively. Lipoxygenases act by degrading linoleic and linolenic acids into volatile aldehydes, such as hexanal (Table 2), while ADH converts volatile aldehydes into alcohols to be subsequently esterified (Yan et al., 2018). Two aldehydes and two alcohols were synthesized in the first stage and then decreased, suggesting a possible conversion into volatile esters. The alcohol 3-hexen-1-ol had a sharp reduction of 99.16 % in area from the first to the second stage, as did the aldehyde 2-hexanal with a reduction of 94.9 % in area, and hexanal was no longer detected. From the immature to the green mature stage, the area of esters increased by 34.31 %, concomitantly with the reduction of their aldehyde and alcohol precursors. This indicates that it is at this stage of development that the production of volatile esters reaches its synthetic peak in *A. crassiflora* Mart.

Table 2
Volatile organic compounds (mean ± standard deviation) in the pulp of *A. crassiflora* Mart. at four stages of development. Different letters indicate significant differences ($p < 0.05$) by ANOVA analysis followed by the Scott-Knott test. RI = retention index calculated. RI Lit = retention index found in literature. ND – Not Detected. NF – Not found.

Compounds	RI	RI Lit	Immature	Mature green	Ripe	Overripe
Esters						
Ethyl butyrate	803	804	ND	0.07±0.01^{c}	0.17±0.01^{a}	0.13±0.00^{b}
Methyl hexanoate	919	921	3.74±0.37^{b}	4.4 ± 0.15^{a}	2.67±0.08^{c}	2.27±0.16^{c}
Ethyl hexanoate	976	998	13.21±0.6^{d}	28.52±0.67^{c}	32.24±0.06^{a}	30.21±0.92^{b}
Hexyl acetate	1013	1014	ND	ND	0.04±0.00^{b}	0.09±0.00^{a}
Ethyl-(3E)-hexenoate	1004	1004	0.19±0.01^{a}	ND	0.02±0.00^{c}	0.08±0.00^{b}
Propyl hexanoate	1112	1097	ND	0.09±0.00^{c}	0.11±0.01^{b}	0.13±0.01^{a}
Methyl octanoate	1124	1123	21.64±1.64^{a}	22.02±0.44^{a}	11.54±0.25^{b}	11.61±0.15^{b}
Ethyl-(4E)-octenoate	1189	1186	ND	ND	1.26±0.06^{a}	1.27±0.01^{a}
Ethyl octanoate	1197	1198	23.09±0.86^{d}	26.22±0.47^{c}	32.76±0.13^{b}	33.85±0.34^{a}
Ethyl (E)−2-octenoate	1248	1249	ND	ND	0.07±0.00^{a}	0.08±0.00^{a}
Isoamyl hexanoate	1251	1249	ND	0.09±0.00^{c}	0.38±0.03^{b}	0.5 ± 0.00^{a}
Methyl decanoate	1292	1324	ND	0.55±0.01^{a}	0.52±0.04^{a}	0.55±0.00^{a}
cis-3-Hexenyl hexanoate	1353	1380	ND	0.12±0.01	ND	ND
Ethyl decanoate	1398	1398	ND	0.44±0.01^{c}	2.9 ± 0.18^{a}	2.55±0.11^{b}
Hexyl hexanoate	1386	1379	ND	ND	0.13±0.00^{b}	0.18±0.00^{a}
Isoamyl octanoate	1447	1445	ND	ND	0.05±0.00^{b}	0.08±0.00^{a}
4-cyano-2.6-diiodophenyl octanoate	1455	NF	ND	0.58±0.01^{b}	1.91±0.00^{a}	1.98±0.11^{a}
Terpenes						
α-pinene	934	939	0.8 ± 0.06	ND	ND	ND
β-pinene	979	981	0.7 ± 0.01	ND	ND	ND
α-Phellandrene	1008	1007	0.33±0.05^{b}	1.76±0.08^{a}	0.02±0.00^{b}	0.08±0.00^{b}
Menthene	1031	1021	1.63±0.04^{a}	0.08±0.00^{b}	0.15±0.03^{b}	0.12±0.02^{b}
β-ocimene	1047	1038	ND	ND	ND	0.06±0.00
Acids						
Butanoic acid	798	820	ND	ND	ND	0.16±0.01
Octanoic acid	1194	1171	5.92±0.44^{a}	6.49±0.22^{a}	1.44±0.04^{b}	1.74±0.13^{b}
Aldehydes						
Hexanal	801	801	0.95±0.09	ND	ND	ND
2-Hexenal	852	854	1.77±0.11^{a}	0.09±0.00^{b}	ND	ND
Alcohols						
3-Hexen-1-ol	854	858	10.76±0.41^{a}	0.09±0.00^{b}	ND	ND
Hexanol	869	870	0.43±0.03^{a}	ND	ND	0.28±0.00^{b}
Others						
Styrene	888	893	0.53±0.05^{a}	0.1 ± 0.01^{b}	0.06±0.00^{b}	0.05±0.00^{b}
Hexanoic anhydride	1259	NF	ND	4.88±0.2^{b}	7.37±0.33^{a}	7.61±0.39^{a}

Terpenes, the second most abundant class in the volatile profile of marolo, showed more intense accumulation between the two initial stages. It is known that terpenes can act as alarm substances, defensive emissions and defense mechanisms against insects and pathogenic microorganisms at different concentrations and toxicity levels (Ninkuu et al., 2021). Three isoforms of 4-hydroxy-3-methylbut-2-en-1-yl diphosphate synthase (HDS, EC:1.17.7.1) were present in the marolo proteome. This is one of the seven enzymes that participate in the MEP pathway, synthesizing monoterpenes at its end. Of these three isoforms, only one showed statistically significant difference between the four stages, with maximum and minimum accumulation in the immature and ripe stages, respectively. Concomitantly, the immature stage had the highest concentration of terpenes, totaling an area of 3.46 %. Another enzyme involved in the synthesis of many terpenes detected was β-sesquiphellandrene synthase (EC:4.2.3.123). Although this is a sesquiterpene synthase, it can form different compounds using farnesyl diphosphate (FPP) or GPP as substrates. When this enzyme uses GPP, it produces up to nine distinct monoterpenes, including α-phellandrene (Zhuang et al., 2012). This terpenoid was the most abundant detected in this class in marolo, with an area of 1.76 % in the mature green stage. The specific terpene synthases of the other compounds identified in this class were not detected in the marolo proteome.

Although the presence of sesquiterpenes (C_{15}), compounds less volatile than monoterpenes, was not detected in our study, the presence of sesquiterpene synthases was remarkable in all stages of the marolo proteome. τ-cadinol synthase (EC:4.2.3.173), Germacrene A synthase (EC:4.2.3.23), Valerena-4,7(11)-diene synthase (EC:4.2.3.139), Valencene synthase (EC:4.2.3.73) and (E,E)-germacrene B synthase (EC:4.2.3.71) were identified. In addition to these, three Farnesyl pyrophosphate synthases (FPS, EC:2.5.1.1) were detected. FPS forms the initial substrates for the action of sesquiterpene synthases (Li et al., 2023b). The presence of this set of proteins suggests a relevant production of marolo sesquiterns throughout the development of the fruit, although not detected.

Octanoic acid (C_8, Table 2) is a short-chain fatty acid (FA) and a precursor to other compounds. FAs have been increasingly demanded in industries for applications such as fuels, cosmetics, pharmaceuticals, food additives, and as precursors to a variety of industrial chemicals, such as alkanes, α-olefins, and fatty acid methyl or ethyl esters (Chen et al., 2018; Wernig et al., 2021). Short-chain FAs, such as octanoic acid, are especially used directly as food preservatives and dietary supplements (Chen et al., 2018). The first step in FA biosynthesis is catalyzed by acetyl-CoA carboxylase (ACCase), converting acetyl-CoA to malonyl-CoA. In the marolo proteome, five ACCase isoforms were detected, two of which had statistically significant accumulation. These two showed greater accumulation in the immature and mature green stages, and less accumulation in the overripe stage. Octanoic acid had a behavior similar to the accumulation of these enzymes, with higher area values in the two initial stages, followed by a sharp decrease of 77.8 % from the second to the third stage. Octanoic acid is reported as a potential fungicide and is toxic to many insects (Dalcin et al., 2022). It is possible that these protective characteristics are related to the fruit in the development phase as a preventive action against biotic stresses that could negatively influence the development of the marolo. The emission of this volatile compound should inhibit the approach of insects, in agreement with the greater presence of terpenes in the initial stages of the marolo, which act in a similar way.

Regarding the compound hexanoic anhydride (Table 2), little is

reported about this metabolite that is formed by the condensation of two hexanoic acid molecules (Woo et al., 2017). Hexanoic acid has functions similar to octanoic acid regarding protection against biotic stresses in plant cells. Therefore, it is possible that this assignment may be related to hexanoic anhydride, although specific studies are needed.

4. Conclusion

Proteomics and metabolomics of *A. crassiflora* Mart. allowed us to observe biochemical changes throughout development. In the immature stage, the action of ribosomal, transcriptional and post-translational proteins was highlighted, evidencing the focus on increasing the protein synthesis machinery to produce more proteins that should coordinate the other biological processes essential for development. Eukaryotic translation initiation factor 5A, eukaryotic initiation factor 4A-9 and spermidine synthase 1 are perhaps the most representative proteins and biomarkers of this biological process at this stage. The GATA, MADS-Box, MYB, F-box and HD-Zip TFs families are important in the regulation of biological processes in marolo, and other processes such as cell wall degradation and the antioxidant system could also be observed by the accumulation of a set of proteins. The ripe marolo fruit was a rich source of bioactive compounds such as vitamin C, carotenoids, alkaloids and phenolic compounds, and the volatile profile of marolo showed supremacy of volatile esters. Many enzymes could be associated with the synthesis and degradation of these secondary metabolites among the four stages. Therefore, proteomics in conjunction with metabolomics allowed us to have a molecular view of how compounds and proteins are produced in marolo development and how the behavior of these molecules appears to influence biological processes and biosynthetic pathways through enzymatic action.

For the future of molecular research on marolo, as well as other fruits, some suggestions are indicated. The first is to perform other metabolomic analyses covering a greater coverage of metabolite groups, which can be related to more proteins already identified. In addition, the application of other omics, such as transcriptomics in integration with proteomics, can fully elucidate the dynamics of gene expression and deeply analyze the effects of positive or negative gene regulation at the post-translational level. With this set of information, more insights for biotechnological applications and cultivation of marolo can be generated, adding value to this species that is so important for the Brazilian Cerrado.

CRediT authorship contribution statement

Carlos Alexandre Rocha da Costa: Writing – original draft, Software, Methodology, Investigation, Data curation, Conceptualization. **Sidney Vasconcelos do Nascimento:** Writing – review & editing, Methodology, Investigation, Data curation. **Rafael Borges da Silva Valadares:** Validation, Methodology, Investigation, Data curation, Conceptualization. **Luíz Guilherme Malaquias da Silva:** Methodology, Investigation. **Gilson Gustavo Lucinda Machado:** Methodology, Investigation. **Alice de Paula de Sousa Cavalcante:** Methodology, Investigation. **Sayure Mariana Raad Nahon:** Methodology, Investigation. **Carlos Henrique Milagres Ribeiro:** Methodology, Investigation. **Grécia de Andrade Souza:** Methodology, Investigation. **Luiz José Rodrigues:** Writing – review & editing. **Elisangela Elena Nunes Carvalho:** Methodology, Conceptualization. **Eduardo Valério de Barros Vilas Boas:** Writing – review & editing, Validation, Supervision, Resources, Project administration, Methodology, Investigation, Conceptualization.

Declaration of competing interest

The authors declare that they have no known competing financial interests or personal relationships that could have appeared to influence the work reported in this paper.

Acknowledgment

The authors would like to thank the Central of Analysis and Chemical Prospecting of the Federal University of Lavras and the Vale Technological Institute for the support.

Funding sources

Funding: This work was supported by the FAPEMIG, Fundação de Amparo à Pesquisa do Estado de Minas Gerais [PPM-00355–17]; Conselho Nacional de Desenvolvimento Científico e Tecnológico [302699/2019–8; 404716/2021–0]; and Coordenação de Aperfeiçoamento de Pessoal de Nível Superior [88881.068456/2014–01; 88881.200497/2018–01].

Supplementary materials

Supplementary material associated with this article can be found, in the online version, at doi:10.1016/j.scienta.2024.113809.

Data availability

Data will be made available on request.

References

Almeida, R.F., Moreno, I.F., Machado, A.P.O., Meireles, M.A.A., da Silva, L.K.F., Batista, E.A.C., 2024. Araticum (*Annona crassiflora* Mart.): a critical review for the food industry. Food Res. Int. 184, 114241. https://doi.org/10.1016/J.FOODRES.2024.114241.

Arias, A., Feijoo, G., Moreira, M.T., 2022. Exploring the potential of antioxidants from fruits and vegetables and strategies for their recovery. Innovat. Food Sci. Emerg. Technol. 77, 102974. https://doi.org/10.1016/J.IFSET.2022.102974.

Arruda, H.S., Borsoi, F.T., Andrade, A.C., Pastore, G.M., Marostica Junior, M.R., 2023. Scientific advances in the last decade on the recovery, characterization, and functionality of bioactive compounds from the araticum fruit (Annona crassiflora Mart.). Plants 12 (7). https://doi.org/10.3390/plants12071536. Vol.

Arruda, H.S., Pereira, G.A., de Morais, D.R., Eberlin, M.N., Pastore, G.M., 2018. Determination of free, esterified, glycosylated and insoluble-bound phenolics composition in the edible part of araticum fruit (Annona crassiflora Mart.) and its by-products by HPLC-ESI-MS/MS. Food Chem. 245, 738–749. https://doi.org/10.1016/J.FOODCHEM.2017.11.120.

Ashihara, H., 2015. Plant biochemistry: trigonelline biosynthesis in coffea arabica and coffea canephora. Coffee Health Dis. Prevent. 19–28. https://doi.org/10.1016/B978-0-12-409517-5.00003-6.

Carvalho, N.C.C., Monteiro, O.S., da Rocha, C.Q., Longato, G.B., Smith, R.E., da Silva, J. K.R., Maia, J.G.S., 2022. Phytochemical analysis of the fruit pulp extracts from *Annona crassiflora* Mart. and evaluation of their antioxidant and antiproliferative activities. Foods. 11 (14). https://doi.org/10.3390/foods11142079.

Chen, Y., Reinhardt, M., Neris, N., Kerns, L., Mansell, T.J., Jarboe, L.R., 2018. Lessons in membrane engineering for octanoic acid production from environmental Escherichia coli isolates. Appl. Environ. Microbiol. 84 (19). https://doi.org/10.1128/AEM.01285-18.

Cunningham, F.X., Gantt, E., 2007. A portfolio of plasmids for identification and analysis of carotenoid pathway enzymes: adonis aestivalis as a case study. Photosyn. Res. 92 (2), 245–259. https://doi.org/10.1007/s11120-007-9210-0.

da Costa, C.A.R., do Nascimento, S.V., da Silva Valadares, R.B., da Silva, L.G.M., Machado, G.G.L., da Costa, I.R.C., Nahon, S.M.R., Rodrigues, L.J., Vilas Boas, E.V., de, B., 2024a. Proteome and metabolome of *Caryocar brasiliense* camb. fruit and their interaction during development. Food Res. Int. 191. https://doi.org/10.1016/j.foodres.2024.114687.

da Costa, C.A.R., Machado, G.G.L., Rodrigues, L.J., de Barros, H.E.A., Natarelli, C.V.L., Boas, E.V., de, B.V., 2023. Phenolic compounds profile and antioxidant activity of purple passion fruit's pulp, peel and seed at different maturation stages. Sci. Hortic. 321, 112244. https://doi.org/10.1016/J.SCIENTA.2023.112244.

da Costa, C.A.R., Pinheiro, F.S., da Silva, L.G.M., da Silva, F.M.O., Toro, M.J.U., 2024b. Evaluation of physicochemical properties, bioactive compounds, and antioxidant activity in traditional and decaffeinated coffee blends from the Cerrado Mineiro Region in Brazil. Food Human. 3, 100388. https://doi.org/10.1016/j.foohum.2024.100388.

da Silva, E.P., Vilas Boas, E.V., de, B., Xisto, A.L.P.R., 2013. Characterization and development of marolo (*Annona crassiflora*, Mart.). Food Sci. Technol. Campinas 33 (4), 666–675.

da Silva, J., Cerdeira, C.D., Chavasco, J.M., Cintra, A.B.P., da Silva, C.B.P., de Mendonça, A.N., Ishikawa, T., Boriollo, M.F.G., Chavasco, J.K., 2014. Triagem in vitro da atividade antibacteriana de Bidens pilosa Linné e Annona crassiflora mart. contra Staphylococcus aureus resistente à oxacilina (ORSA) provenientes do

ambiente aéreo na clínica odontológica. Rev. Inst. Med. Trop. Sao Paulo 56 (4), 333–340. https://doi.org/10.1590/S0036-46652014000400011.
Dalcin, M.S., Dias, B.L., Viteri Jumbo, L.O., Oliveira, A.C.S.S., Araújo, S.H.C., Moura, W. S., Mourão, D.S.C., Ferreira, T.P.S., Campos, F.S., Cangussu, A.S.R., Alves, M.V.G., Andrade, B.S., Mantilla-Afanador, J.G., Aguiar, R.W.A., Oliveira, E.E., Santos, G.R., 2022. Potential action mechanism and inhibition efficacy of *Morinda citrifolia* essential oil and octanoic acid against stagonosporopsis cucurbitacearum infestations. Molecules. 27 (16). https://doi.org/10.3390/molecules27165173.
Dhanalakshmi, M., Sruthi, D., Jinuraj, K.R., Das, K., Dave, S., Andal, N.M., Das, J., 2023. Mannose: a potential saccharide candidate in disease management. Med. Chem. Res. 32 (3), 391–408. https://doi.org/10.1007/s00044-023-03015-z.
do Nascimento, S.V., Costa, P.H., de, O., Herrera, H., Caldeira, C.F., Gastauer, M., Ramos, S.J., Oliveira, G., Valadares, R.B., da, S., 2022. Proteomic profiling and rhizosphere-associated microbial communities reveal adaptive mechanisms of *Dioclea apurensis* Kunth in Eastern Amazon's rehabilitating minelands. Plants 11 (5). https://doi.org/10.3390/plants11050712.
Fakih, Z., Plourde, M.B., Germain, H., 2023. Differential participation of plant ribosomal proteins from the small ribosomal subunit in protein translation under stress. Biomolecules. 13 (7). https://doi.org/10.3390/biom13071160.
Feng, D., Gao, L., Zheng, Y., Li, D., Zhou, P., 2020. Molecular cloning and function characterisation of a cytoplasmic fructose-1, 6-bisphosphate aldolase gene from coconut (*Cocos nucifera* L.). J. Hortic. Sci. Biotechnol. 1–9. https://doi.org/10.1080/14620316.2020.1749139.
Fonseca, M.R.S., Uagoda, R., Chaves, H.M.L., 2021. Rates, factors, and tolerances of water erosion in the cerrado Biome (Brazil): a meta-analysis of runoff plot data. Earth Surf. Process. Landformes 47, 582–595. https://doi.org/10.1002/esp.5273.
Forlani, S., Mizzotti, C., Masiero, S., 2021. The NAC side of the fruit: tuning of fruit development and maturation. BMC Plant Biol. 21 (1). https://doi.org/10.1186/s12870-021-03029-y.
Gao, F., Mei, X., Li, Y., Guo, J., Shen, Y., 2021. Update on the roles of polyamines in fleshy fruit ripening, senescence, and quality. Front. Plant Sci. 12. https://doi.org/10.3389/fpls.2021.610313.
Gou, N., Zhu, X., Yin, M., Zhao, H., Bai, H., Jiang, N., Xu, W., Wang, C., Zhang, Y., Wuyun, T., 2024. 15-cis-phytoene desaturase and 15-cis-phytoene synthase can catalyze the synthesis of β-carotene and influence the color of apricot pulp. Foods. 13 (2). https://doi.org/10.3390/foods13020300.
Gu, C., Guo, Z.H., Cheng, H.Y., Zhou, Y.H., Qi, K.J., Wang, G.M., Zhang, S.L., 2019. A HD-ZIP II HOMEBOX transcription factor, PpHB.G7, mediates ethylene biosynthesis during fruit ripening in peach. Plant Sci. 278, 12–19. https://doi.org/10.1016/J.PLANTSCI.2018.10.008.
Han, M., Zhang, C., Suglo, P., Sun, S., Wang, M., Su, T., 2021. L-Aspartate: an essential metabolite for plant growth and stress acclimation. Molecules. 26 (7), 1887. https://doi.org/10.3390/molecules26071887.
Hu, L., Tu, B., Yang, W., Yuan, H., Li, J., Guo, L., Zheng, L., Chen, W., Zhu, X., Wang, Y., Qin, P., Ma, B., Li, S., 2020. Mitochondria-associated pyruvate kinase complexes regulate grain filling in rice. Plant Physiol. 183 (3), 1073–1087. https://doi.org/10.1104/pp.20.00279.
Huan, C., Jiang, L., An, X., Yu, M., Xu, Y., Ma, R., Yu, Z., 2016. Potential role of reactive oxygen species and antioxidant genes in the regulation of peach fruit development and ripening. Plant Physiol. Biochem. 104, 294–303. https://doi.org/10.1016/J.PLAPHY.2016.05.013.
Huang, X., Wu, Y., Zhang, S., Yang, H., Wu, W., Lyu, L., Li, W., 2023. Changes in antioxidant substances and antioxidant enzyme activities in raspberry fruits at different developmental stages. Sci. Hortic. 321, 112314. https://doi.org/10.1016/J.SCIENTA.2023.112314.
Institute of Medicine, 2000. Dietary Reference Intakes for Vitamin C, Vitamin E, Selenium, and Carotenoids. The National Academies Press, Washington, DC. https://doi.org/10.17226/9810.
Jiménez-Bremont, J.F., González-Pérez, E., Ortega-Amaro, M.A., Madrigal-Ortiz, S., Duque-Ortiz, A., Mendoza-Mendoza, A., 2024. Volatile organic compounds emitted by Trichoderma: small molecules with biotechnological potential. Sci. Hortic. 325, 112656. https://doi.org/10.1016/J.SCIENTA.2023.112656.
Krause, T., Wiesinger, P., González-Cabanelas, D., Lackus, N., Köllner, T.G., Klüpfel, T., Williams, J., Rohwer, J., Gershenzon, J., Schmidt, A., 2023. HDR, the last enzyme in the MEP pathway, differently regulates isoprenoid biosynthesis in two woody plants. Plant Physiol. 192 (2), 767–788. https://doi.org/10.1093/plphys/kiad110.
Kravchenko, O.v., Baymukhametov, T.N., Afonina, Z.A., Vassilenko, K.S., 2023. High-resolution structure and internal mobility of a plant 40S ribosomal subunit. Int. J. Mol. Sci. 24 (24). https://doi.org/10.3390/ijms242417453.
Le, T.M., La, H.V., Chu, H.D., Ha, Q.T., Quynh, L.T.N., Huyen, T.T.T., Tien, T.van, Gioi, D.H., Pham, M.H., Tran, V.T., Chu, T.B.N., Cao, P.B, 2024. Genome-wide analysis of GATA transcription factor family in quinoa (Chenopodium quinoa): identification, characterization, and expression profiles. J. Trop. Life Sci. 14 (02), 217–228. https://doi.org/10.11594/jtls.14.02.02.
Lepelley, M., Cheminade, G., Tremillon, N., Simkin, A., Caillet, V., McCarthy, J., 2007. Chlorogenic acid synthesis in coffee: an analysis of CGA content and real-time RT-PCR expression of HCT, HQT, C3H1, and CCoAOMT1 genes during grain development in C. canephora. Plant Sci. 172 (5), 978–996. https://doi.org/10.1016/J.PLANTSCI.2007.02.004.
Li, C., Lu, X., Xu, J., Liu, Y., 2023a. Regulation of fruit ripening by MADS-box transcription factors. Sci. Hortic. 314, 111950. https://doi.org/10.1016/J.SCIENTA.2023.111950.
Li, J., Wang, Y., Suh, J.H., 2022. Multi-omics approach in tea polyphenol research regarding tea plant growth, development and tea processing: current technologies and perspectives. Food Sci. Hum. Wellness 11 (3), 524–536. https://doi.org/10.1016/J.FSHW.2021.12.010.
Li, Q.H., Yang, S.P., Yu, Y.N., Khan, A., Feng, P.L., Ali, M., Shao, D., kui, Wang, Y.Y., Zhang, R.X., Gai, W.X., Han, R., Ma, X., Hou, Q.G., Gong, Z.H., 2021. Comprehensive transcriptome-based characterization of differentially expressed genes involved in carotenoid biosynthesis of different ripening stages of Capsicum. Sci. Hortic. 288. https://doi.org/10.1016/j.scienta.2021.110311.
Li, X., Qi, L., Zang, N., Zhao, L., Sun, Y., Huang, X., Wang, H., Yin, Z., Wang, A., 2022a. Integrated metabolome and transcriptome analysis of the regulatory network of volatile ester formation during fruit ripening in pear. Plant Physiol. Biochem. 185, 80–90. https://doi.org/10.1016/J.PLAPHY.2022.04.030.
Li, X., Wang, X., Zhang, Y., Zhang, A., You, C.X., 2022b. Regulation of fleshy fruit ripening: from transcription factors to epigenetic modifications. Hortic Res. 9. https://doi.org/10.1093/hr/uhac013.
Li, Y., Gao, Y., Deng, L., Lian, H., Guo, W., Wu, W., Xue, B., Li, B., Su, Y., Zhang, H., 2023b. Volatile profiling and transcriptome sequencing provide insights into the biosynthesis of α-Pinene and β-Pinene in Liquidambar formosana hance leaves. Genes (Basel) 14 (1). https://doi.org/10.3390/genes14010163.
Li, Z., Zhou, B., Zheng, T., Zhao, C., Shen, X., Wang, X., Qiu, M., Fan, J., 2023c. Integrating metabolomics and proteomics technologies provides insights into the flavor precursor changes at different maturity stages of arabica coffee cherries. Foods. 12 (7). https://doi.org/10.3390/foods12071432.
Lin, Z., Hong, Y., Yin, M., Li, C., Zhang, K., Grierson, D., 2008. A tomato HD-Zip homeobox protein, LeHB-1, plays an important role in floral organogenesis and ripening. Plant J. 55 (2), 301–310. https://doi.org/10.1111/j.1365-313X.2008.03505.x.
Liu, J., Zhang, J., Zhang, J., Miao, H., Wang, J., Gao, P., Hu, W., Jia, C., Wang, Z., Xu, B., Jin, Z., 2017. Genome-wide analysis of banana MADS-box family closely related to fruit development and ripening. Sci Rep 7 (1). https://doi.org/10.1038/s41598-017-03897-1.
Liu, W., Feng, Y., Yu, S., Fan, Z., Li, X., Li, J., Yin, H., 2021. The flavonoid biosynthesis network in plants. Int. J. Mol. Sci. 22 (23). https://doi.org/10.3390/ijms222312824.
Lucas dos Santos, E., Leite, N., Alves de Araújo, L.C., Giffoni de Carvalho, J.T., Souza, K. de P., 2018. Protective effect of Annona crassiflora on oxidative stress and Alzheimer's models in Caenorhabditis elegans. Free Rad. Biol. Med. 128, S125. https://doi.org/10.1016/J.FREERADBIOMED.2018.10.307.
Luo, F., Yan, P., Xie, L., Li, S., Zhu, T., Han, S., Lin, T., Li, S., 2022. Molecular mechanisms of phenylpropane-synthesis-related genes regulating the shoot blight resistance of bambusa pervariabilis × Dendrocalamopsis grandis. Int J Mol Sci 23 (12). https://doi.org/10.3390/ijms23126760.
Marcolino, E., Salavarria, D., da Silva, L.G.M., Almeida, A., Oliveira da Silva, F.M., Ribeiro, C., Dias, J., 2024. Valorization of baobab seeds (Adansonia digitata) as a coffee-like beverage: evaluation of roasting time on bioactive compounds. J. Food Sci. Technol. 61 (4), 727–733. https://doi.org/10.1007/s13197-023-05873-2.
Meira, A.C.F.D.O., Morais, L.C.de, Figueiredo, J.D.A., Veríssimo, L.A.A., Botrel, D.A., Resende, J.V.de, 2023. Microencapsulation of β-carotene using barley residue proteins from beer waste as coating material. J. Microencapsul. 40 (3), 171–185. https://doi.org/10.1080/02652048.2023.2183277.
Momo, J., Rawoof, A., Kumar, A., Islam, K., Ahmad, I., Ramchiary, N., 2022. Proteomics of reproductive development, fruit ripening, and stress responses in tomato. *J. Agric. Food Chem.*. Am. Chem. Soc. https://doi.org/10.1021/acs.jafc.2c06564.
Monribot-Villanueva, J.L., Altúzar-Molina, A., Aluja, M., Zamora-Briseño, J.A., Elizalde-Contreras, J.M., Bautista-Valle, M.v., Arellano de los Santos, J., Sánchez-Martínez, D. E., Rivera-Reséndiz, F.J., Vázquez-Rosas-Landa, M., Camacho-Vázquez, C., Guerrero-Analco, J.A., Ruiz-May, E., 2022. Integrating proteomics and metabolomics approaches to elucidate the ripening process in white Psidium guajava. Food Chem 367, 130656. https://doi.org/10.1016/J.FOODCHEM.2021.130656.
Mostafa, S., Wang, Y., Zeng, W., Jin, B., 2022. Floral scents and fruit aromas: functions, compositions, biosynthesis, and regulation. Front Plant Sci. 13. https://doi.org/10.3389/fpls.2022.860157.
Ninkuu, V., Zhang, L., Yan, J., Fu, Z., Yang, T., Zeng, H., 2021. Biochemistry of terpenes and recent advances in plant protection. Int. J. Mol. Sci. 22 (11), 5710. https://doi.org/10.3390/ijms22115710.
Nishigaki, N., Yoshimi, Y., Kuki, H., Kunieda, T., Hara-Nishimura, I., Tsumuraya, Y., Takahashi, D., Dupree, P., Kotake, T., 2021. Galactoglucomannan structure of Arabidopsis seed-coat mucilage in GDP-mannose synthesis impaired mutants. Physiol. Plant. 173 (3), 1244–1252. https://doi.org/10.1111/ppl.13519.
Pálfi, P., Bakacsy, L., Kovács, H., Szepesi, Á., 2021. Hypusination, a metabolic posttranslational modification of eif5a in plants during development and environmental stress responses. Plants 10 (7). https://doi.org/10.3390/plants10071261.
Park, J., Pandya, V.R., Ezekiel, S.J., Berghuis, A.M., 2021. Phosphonate and bisphosphonate inhibitors of farnesyl pyrophosphate synthases: a structure-guided perspective. Front. Chem. 8. https://doi.org/10.3389/fchem.2020.612728.
Park, M.H., Wolff, E.C., 2018. Hypusine, a polyamine-derived amino acid critical for eukaryotic translation. J. Biol. Chem. 293 (48), 18710–18718. https://doi.org/10.1074/jbc.TM118.003341.
Ramos, A.L.C.C., Mazzinghy, A.C.do C., Correia, V.T.da V., Nunes, B.V., Ribeiro, L.V., Silva, V.D.M., Weichert, R.F., Paula, A.C.C.F.F.de, Sousa, I.M.N.de, Ferreira, R.M.de S.B., Batista-Santos, P., Araújo, R.L.B.de, Melo, J.O.F, 2022. An integrative approach to the flavonoid profile in some plants' parts of the annona genus. Plants 11 (21). https://doi.org/10.3390/plants11212855.
Ramos, A.L.C.C., Minighin, E.C., Soares, I.I.C., Ferreira, R.M.de S.B., Sousa, I.M.N.de, Augusti, R., Labanca, R.A., Araújo, R.L.B.de, Melo, J.O.F, 2023. Evaluation of the total phenolic content, antioxidative capacity, and chemical fingerprint of Annona crassiflora Mart. Bioaccessible molecules. Food Res. Int. 165, 112514. https://doi.org/10.1016/J.FOODRES.2023.112514.

Randhawa, M.A., Javed, M.S., Ahmad, Z., Amjad, A., Khan, A.A., Shah, F.U.H., Filza, F., 2020. Amassing of hydroxymethylfurfural, 2-furfural and 5-methyl furfural in orange (Citrus reticulata) juice during storage. Food Sci. Technol. (Brazil) 40 (2), 382–386. https://doi.org/10.1590/fst.41718.

Rodriguez-Amaya, D.B., 2001. A Guide to Carotenoid Analysis in Foods, 1th ed. ILSI Press.

Rosan Fortunato Seixas, F., Kempfer Bassoli, B., Borghi Virgolin, L., Chancare Garcia, L., Soares Janzantti, N., 2021. Physicochemical properties and effects of fruit pulps from the amazon biome on physiological parameters in rats. Nutrients. 13 (5). https://doi.org/10.3390/nu13051484.

Saha, A., Das, S., Moin, M., Dutta, M., Bakshi, A., Madhav, M.S., Kirti, P.B., 2017. Genome-wide identification and comprehensive expression profiling of ribosomal protein small subunit (RPS) genes and their comparative analysis with the large subunit (RPL) genes in rice. Front. Plant Sci. 8. https://doi.org/10.3389/fpls.2017.01553.

Sánchez-Gómez, C., Posé, D., Martín-Pizarro, C., 2022. Insights into transcription factors controlling strawberry fruit development and ripening. Front. Plant Sci. 13. https://doi.org/10.3389/fpls.2022.1022369.

Sathasivam, R., Radhakrishnan, R., Kim, J.K., Park, S.U., 2021. An update on biosynthesis and regulation of carotenoids in plants. South Afric. J. Bot. 140, 290–302. https://doi.org/10.1016/J.SAJB.2020.05.015.

Stafussa, A.P., Maciel, G.M., Bortolini, D.G., Maroldi, W.V., Ribeiro, V.R., Fachi, M.M., Pontarolo, R., Bach, F., Pedro, A.C., Haminiuk, C.W.I., 2021. Bioactivity and bioaccessibility of phenolic compounds from Brazilian fruit purees. Future Foods. 4, 100066. https://doi.org/10.1016/J.FUFO.2021.100066.

Strohecker, R., Henning, H.M., 1967. Análisis de Vitaminas: Métodos Comprobados, 1th ed. Paz Montalvo.

Sutaoney, P., Rai, S.N., Sinha, S., Choudhary, R., Gupta, A.K., Singh, S.K., Banerjee, P., 2024. Current perspective in research and industrial applications of microbial cellulases. Int. J. Biol. Macromol. 264, 130639. https://doi.org/10.1016/J.IJBIOMAC.2024.130639.

Tang, H., Zhang, X., Gong, B., Yan, Y., Shi, Q., 2020. Proteomics and metabolomics analysis of tomato fruit at different maturity stages and under salt treatment. Food Chem 311, 126009. https://doi.org/10.1016/J.FOODCHEM.2019.126009.

Tartaglia, M., Zuzolo, D., Prigioniero, A., Ranauda, M.A., Scarano, P., Tienda-Parrilla, M., Hernandez-Lao, T., Jorrín-Novo, J., Guarino, C., 2024. Changes in the proteomics and metabolomics profiles of Cormus Domestica (L.) fruits during the ripening process. BMC Plant Biol. 24 (1), 945. https://doi.org/10.1186/s12870-024-05677-2.

Tian, L., Zhao, X., Hu, Z., Liu, J., Ma, J., Fan, Y., Liu, D., 2024. iTRAQ-based proteomics identifies proteins associated with betaine accumulation in Lycium barbarum L. J. Proteomic. 290, 105033. https://doi.org/10.1016/J.JPROT.2023.105033.

Utpott, M., Rodrigues, E., Rios, A., de, O., Mercali, G.D., Flôres, S.H., 2022. Metabolomics: an analytical technique for food processing evaluation. Food Chem. 366, 130685. https://doi.org/10.1016/J.FOODCHEM.2021.130685.

Wang, X., Tang, Y., Huang, H., Wu, D., Chen, X., Li, J., Zheng, H., Zhan, R., Chen, L., 2022. Functional analysis of Pogostemon cablin farnesyl pyrophosphate synthase gene and its binding transcription factor PcWRKY44 in regulating biosynthesis of patchouli alcohol. Front. Plant Sci. 13. https://doi.org/10.3389/fpls.2022.946629.

Wernig, F., Baumann, L., Boles, E., Oreb, M., 2021. Production of octanoic acid in Saccharomyces cerevisiae: investigation of new precursor supply engineering strategies and intrinsic limitations. Biotechnol. Bioeng. 118 (8), 3046–3057. https://doi.org/10.1002/bit.27814.

Woo, Y., Lee, Y., Choi, J.W., Suh, D.J., Lee, C.H., Ha, J.M., Park, M.J., 2017. Role of anhydride in the ketonization of carboxylic acid: kinetic study on dimerization of hexanoic acid. Ind. Eng. Chem. Res. 56 (4), 872–880. https://doi.org/10.1021/acs.iecr.6b04605.

Xu, K., Wu, N., Yao, W., Li, X., Zhou, Y., Li, H., 2021. The biological function and roles in phytohormone signaling of the f-box protein in plants. Agronomy 11 (11). https://doi.org/10.3390/agronomy11112360.

Xu, Y., Zhao, J., Liu, X., Zhang, C., Zhao, Z., Li, X., Sun, B., 2022. Flavor mystery of Chinese traditional fermented baijiu: the great contribution of ester compounds. Food Chem. 369, 130920. https://doi.org/10.1016/j.foodchem.2021.130920.

Yan, J., Ban, Z., Lu, H., Li, D., Poverenov, E., Luo, Z., Li, L., 2018. The aroma volatile repertoire in strawberry fruit: a review. J. Sci. Food Agric. 98 (12), 4395–4402. https://doi.org/10.1002/jsfa.9039.

Yang, Y., Jiang, M., Feng, J., Wu, C., Shan, W., Kuang, J., Chen, J., Hu, Z., Lu, W., 2021. Transcriptome analysis of low-temperature-affected ripening revealed MYB transcription factors-mediated regulatory network in banana fruit. Food Res. Int. 148. https://doi.org/10.1016/j.foodres.2021.110616.

Yu, C., Yan, M., Dong, H., Luo, J., Ke, Y., Guo, A., Chen, Y., Zhang, J., Huang, X., 2021. Maize bHLH55 functions positively in salt tolerance through modulation of AsA biosynthesis by directly regulating GDP-mannose pathway genes. Plant Sci. 302, 110676. https://doi.org/10.1016/J.PLANTSCI.2020.110676.

Zheng, X., Gong, M., Zhang, Q., Tan, H., Li, L., Tang, Y., Li, Z., Peng, M., Deng, W., 2022. Metabolism and regulation of ascorbic acid in fruits. Plants 11 (12), 1602. https://doi.org/10.3390/plants11121602.

Zhou, P., Yue, C., Zhang, Y., Li, Y., Da, X., Zhou, X., Ye, L., 2022. Alleviation of the byproducts formation enables highly efficient biosynthesis of rosmarinic acid in saccharomyces cerevisiae. J. Agric. Food Chem. 70 (16), 5077–5087. https://doi.org/10.1021/acs.jafc.2c01179.

Zhuang, X., Köllner, T.G., Zhao, N., Li, G., Jiang, Y., Zhu, L., Ma, J., Degenhardt, J., Chen, F., 2012. Dynamic evolution of herbivore-induced sesquiterpene biosynthesis in sorghum and related grass crops. Plant J. 69 (1), 70–80. https://doi.org/10.1111/j.1365-313X.2011.04771.x.